

A COMBINED DISSOCIATIVE AND KICK-OUT DIFFUSION MODEL WITH CHARGE EFFECTS, PART II: OUT-DIFFUSION

By

J.R. KING

School of Mathematical Sciences, University of Nottingham

and

M.G. MEERE*

Department of Mathematical Physics, National University of Ireland, Galway

[Received 19 May 1999. Read 30 November 2000. Published 30 August 2002.]

ABSTRACT

This paper considers a new combined dissociative and kick-out diffusion model subject to boundary and initial conditions that model out-diffusion. Both asymptotic and numerical solutions are presented, and the transition from dissociative to kick-out behaviour is studied. Noteworthy components of the asymptotically reduced problems include a number of novel non-local diffusion equations. A related initial-boundary value problem for the porous medium equation is outlined to highlight and clarify some of the key features of the analysis in the context of a much simpler model.

1. Introduction

In this paper we study a combined dissociative and kick-out diffusion model subject to boundary and initial conditions that model out-diffusion. The paper is the second of a pair, the first of which (J.R. King and M.G. Meere, in this volume, pp 49–78, hereafter ‘Part I’) considers in-diffusion. In Part I the relevant model is derived and discussed in some detail, so the background need not be reproduced here. The dimensional form for the system of equations that we study is

$$\begin{aligned}k_{dL}sp^{\alpha+\mu+1} &= k_{dR}iV, & k_{kL}sp^{\alpha-\nu+1} &= k_{kR}i, \\ \frac{\partial}{\partial t}(s+i) &= D_i \frac{\partial}{\partial x} \left(\frac{\partial i}{\partial x} - \alpha \frac{i}{p} \frac{\partial p}{\partial x} \right), \\ \frac{\partial}{\partial t}(V-I+s) &= D_V \frac{\partial}{\partial x} \left(\frac{\partial V}{\partial x} - \mu \frac{V}{p} \frac{\partial p}{\partial x} \right) - D_I \frac{\partial}{\partial x} \left(\frac{\partial I}{\partial x} - \nu \frac{I}{p} \frac{\partial p}{\partial x} \right), \\ p &= \frac{1}{2} \left(s - \alpha i - \mu V - \nu I + \sqrt{(s - \alpha i - \mu V - \nu I)^2 + 4n_i^2} \right),\end{aligned}\tag{1.1}$$

where $s(x, t)$, $i(x, t)$, $V(x, t)$, $I(x, t)$ and $p(x, t)$ are the concentrations of substitutional impurity, interstitial impurity, vacancies, self-interstitials and holes, respectively, at

* Corresponding author, e-mail: martin.meere@nuigalway.ie

distance $x > 0$ into the semiconductor and time $t > 0$. The rate constants for the dissociative reaction have been denoted by k_{dL} and k_{dR} , while those for kick-out are k_{kL} and k_{kR} . The quantities D_i , D_V and D_I denote the diffusivities of the interstitial impurity, vacancies and self-interstitials and are all constant. Finally, we have denoted by α , μ and ν the charges on, respectively, interstitial impurity atoms, vacancies and self-interstitials and by n_i the intrinsic concentration of holes and electrons.

The layout of the analysis presented in this paper follows that of Part I, the principal difference being that we are using different boundary and initial conditions, which, as we shall see, lead to significant differences in behaviour. As in Part I, we consider two sets of charge states, namely, (I) the neutral defect model with $\mu = \nu = 0$, $\alpha = 1$; (II) the charged defect model with $\mu = 0$, $\nu = 2$ and $\alpha = 1$. Some references to experimental and modelling work that motivates these choices can be found in Part I.

Out-diffusion (as discussed by Yu *et al.* [3], for example) occurs when a semiconductor wafer into which impurity has previously been diffused is placed in an environment such that the impurity (no source of which is present) is able to leave the wafer through its surface. The simplest boundary and initial conditions describing such a process are

$$\begin{aligned} i &= 0, & V &= V^* & \text{on } x &= 0, \\ i &\rightarrow i^*, & V &\rightarrow V^* & \text{as } x &\rightarrow +\infty, \\ i &= i^*, & V &= V^* & \text{at } t &= 0, \end{aligned}$$

where i^* is the initial concentration of impurity interstitials in the bulk and V^* is the equilibrium vacancy concentration. We thus take the semiconductor surface ($x = 0$) to be a perfect sink for impurity that maintains point defect equilibrium. Uniform initial conditions are adopted as the simplest possible choice; they enable the relevant phenomena to be identified, and the resulting analysis describes the small-time behaviour for much more general initial data. Our asymptotic and numerical approaches can readily be generalised to other cases.

The non-dimensionalisation we adopt is similar to that used for the in-diffusion case in Part I. The only change is that here we denote by s^* , I^* and p^* the concentrations of substitutionals, self-interstitials and holes as $x \rightarrow +\infty$, and the non-dimensional equations for the neutral defect case (I) are (see Part I)

$$\begin{aligned} sp^2 &= iV, & sIp^2 &= i, \\ \frac{\partial}{\partial t}(s + \lambda i) &= \lambda \frac{\partial}{\partial x} \left(\frac{\partial i}{\partial x} - \frac{i}{p} \frac{\partial p}{\partial x} \right), \\ \frac{\partial}{\partial t}(\delta V - \varepsilon I + s) &= \beta \delta \frac{\partial^2 V}{\partial x^2} - \gamma \varepsilon \frac{\partial^2 I}{\partial x^2}, \\ p &= \frac{s - \lambda i + \sqrt{(s - \lambda i)^2 + 4\varpi^2}}{1 - \lambda + \sqrt{(1 - \lambda)^2 + 4\varpi^2}}, \end{aligned} \tag{1.2}$$

where we have dimensionless parameters

$$\lambda = \frac{i^*}{s^*}, \quad \delta = \frac{V^*}{s^*}, \quad \varepsilon = \frac{I^*}{s^*}, \quad \beta = \frac{D_V}{D_i}, \quad \gamma = \frac{D_I}{D_i}, \quad \varpi = \frac{n_i}{s^*}.$$

These equations are to be solved subject to the non-dimensional boundary and initial conditions

$$\begin{aligned} i &= 0, & V &= 1 & \text{on } x &= 0, \\ i &\rightarrow 1, & V &\rightarrow 1 & \text{as } x &\rightarrow +\infty, \\ i &= 1, & V &= 1 & \text{at } t &= 0. \end{aligned} \tag{1.3}$$

For the charged defect case (II), I^* is replaced by $I_s^* \equiv I^*(p^*/n_i)^2$ in the definition of ε , and the non-dimensional equations are then (see Part I)

$$\begin{aligned} sp^2 &= iV, & sI &= i, \\ \frac{\partial}{\partial t}(s + \lambda i) &= \lambda \frac{\partial}{\partial x} \left(\frac{\partial i}{\partial x} - \frac{i}{p} \frac{\partial p}{\partial x} \right), \\ \frac{\partial}{\partial t}(\delta V - \varepsilon I + s) &= \beta \delta \frac{\partial^2 V}{\partial x^2} - \gamma \varepsilon \frac{\partial}{\partial x} \left(\frac{\partial I}{\partial x} - \frac{2I}{p} \frac{\partial p}{\partial x} \right), \\ p &= \frac{s - \lambda i - 2\varepsilon I + \sqrt{(s - \lambda i - 2\varepsilon I)^2 + 4\varpi^2}}{1 - \lambda - 2\varepsilon + \sqrt{(1 - \lambda - 2\varepsilon)^2 + 4\varpi^2}}, \end{aligned} \tag{1.4}$$

together with (1.3). It is worth mentioning here the conditions that the other species s, I and p satisfy. These can be deduced from (1.3) and the algebraic relations in (1.2) or (1.4). We have for neutral defects

$$\begin{aligned} s &= 0, & I &= 1, & p &= \theta_1 & \text{on } x &= 0, \\ s &\rightarrow 1, & I &\rightarrow 1, & p &\rightarrow 1 & \text{at } x &\rightarrow +\infty, \\ s &= 1, & I &= 1, & p &= 1 & \text{at } t &= 0 \end{aligned}$$

and for charged defects

$$\begin{aligned} s &= 0, & I &= \theta_2^2, & p &= \theta_2 & \text{on } x &= 0, \\ s &\rightarrow 1, & I &\rightarrow 1, & p &\rightarrow 1 & \text{as } x &\rightarrow +\infty, \\ s &= 1, & I &= 1, & p &= 1 & \text{at } t &= 0, \end{aligned}$$

where θ_1 and θ_2 are defined in Part I, being of $O(\varpi)$ as $\varpi \rightarrow 0$. In the asymptotic analysis we set $\varpi = \theta_1 = \theta_2 = 0$, since ϖ is typically extremely small in practice.

The solutions to the problems considered in this paper are self-similar, with

$$s = s(x/\sqrt{t}), \quad i = i(x/\sqrt{t}), \quad p = p(x/\sqrt{t}), \quad I = I(x/\sqrt{t}), \quad V = V(x/\sqrt{t}), \tag{1.5}$$

so that they may reformulated as boundary value problems for coupled systems of

ordinary differential equations. However, as remarked in Part I, this reformulation is of limited value in the present context, and we retain the systems in their original form. The information contained in (1.5) can nevertheless sometimes be useful in shortening the analysis.

In practice, ε and δ are typically very small quantities; this will be exploited in what follows by applying singular perturbation methods. We note that the out-diffusion problems for the pure dissociative ($\varepsilon = 0$) and pure kick-out ($\delta = 0$) cases have not previously been analysed, and these are treated below as special cases.

2. Numerical methods

The numerical procedure is essentially the same as that used for the in-diffusion problems; see Part I. The principal difference here is that we now use backward difference approximations for the first derivatives in x . Using backward differences to approximate the $\partial i/\partial x$ term corresponds to upwinding, since the coefficient of $\partial i/\partial x$ when brought to the left-hand side of (1.4)₂ is the positive quantity $\lambda \partial(\ln p)/\partial x$; a similar comment applies to the backward difference approximations for $\partial I/\partial x$. Numerical solutions obtained by this procedure are given below. Another noteworthy feature is that omitting the εI term in the expression for the holes in the charged defect model (cf. Part I) here involves no leading order loss of accuracy as $\varepsilon \rightarrow 0$, for reasons that will be made clear by the subsequent asymptotic analysis.

3. The neutral defect model

3.1. Outer region, $x = O(1)$

We now consider the solution to (1.2) subject to the conditions (1.3); henceforth, since ϖ is in practice negligible and $\lambda < 1$ holds, we use the simplified expression $p = (s - \lambda i)/(1 - \lambda)$ for the holes (see Part I). As for the in-diffusion problem, we discuss dissociative, kick-out and combined models separately. In terms of the asymptotics, these correspond respectively to the cases $\varepsilon = 0$ with $\delta \rightarrow 0$, $\delta = 0$ with $\varepsilon \rightarrow 0$ and the two transition scalings that are needed, namely, (A) $\varepsilon = O(\delta^{\frac{5}{8}})$ and (B) $\varepsilon = O(\delta^{\frac{3}{4}})$, with $\delta \rightarrow 0$. The leading order outer analysis is identical in all cases, and we discuss this first.

In $x = O(1)$, s, i, p, I and V are all $O(1)$, and we pose

$$s \sim s_0(x, t), \quad i \sim i_0(x, t), \quad p \sim p_0(x, t), \quad I \sim I_0(x, t), \quad V \sim V_0(x, t)$$

as $\varepsilon, \delta \rightarrow 0$ to obtain the leading order equations

$$\begin{aligned} i_0 &= s_0 I_0 p_0^2, & p_0 &= \frac{s_0 - \lambda i_0}{1 - \lambda}, & I_0 V_0 &= 1, \\ \frac{\partial}{\partial t}(s_0 + \lambda i_0) &= \lambda \frac{\partial}{\partial x} \left(\frac{\partial i_0}{\partial x} - \frac{i_0}{p_0} \frac{\partial p_0}{\partial x} \right), & \frac{\partial s_0}{\partial t} &= 0. \end{aligned} \quad (3.1)$$

Integrating the last of these equations yields $s_0 = 1$, so that

$$p_0 = \frac{1 - \lambda i_0}{1 - \lambda}, \quad I_0 = \frac{(1 - \lambda)^2 i_0}{(1 - \lambda i_0)^2}, \quad V_0 = \frac{(1 - \lambda i_0)^2}{(1 - \lambda)^2 i_0}, \quad (3.2)$$

and the penultimate equation appearing in (3.1) can then be written as

$$\frac{\partial i_0}{\partial t} = \frac{\partial}{\partial x} \left(\frac{1}{1 - \lambda i_0} \frac{\partial i_0}{\partial x} \right), \quad (3.3)$$

which is to be solved subject to

$$i_0 = 0 \quad \text{on} \quad x = 0, \quad i_0 \rightarrow 1 \quad \text{as} \quad x \rightarrow +\infty, \quad i_0 = 1 \quad \text{at} \quad t = 0. \quad (3.4)$$

The leading order outer problem is now completely specified (indeed, the similarity ordinary differential equation derived from (3.3) can in fact be integrated exactly (see Crank [2]), although the result is too complicated to be of value here). It is convenient to introduce the positive quantity $J(t)$ defined by

$$J(t) \equiv \lim_{x \rightarrow 0} \left(\frac{\partial i_0}{\partial x} - \frac{i_0}{p_0} \frac{\partial p_0}{\partial x} \right) = \lim_{x \rightarrow 0} \frac{\partial i_0}{\partial x}, \quad (3.5)$$

which is determined as part of the solution to (3.3)–(3.4). The remainder of the analysis considers the behaviour near the surface, and we must now distinguish between the various cases.

3.2. Dissociative model

For $\varepsilon = 0$, $\delta \rightarrow 0$, there are two surface regions to consider, one with $x = O(\delta^{1/3})$ (the inner region) and an even narrower one with $x = O(\delta^{2/3})$ (the inner inner region). A numerical solution illustrating the behaviour of the dissociative model is displayed in Fig. 1. The self-interstitials decouple from the problem, being given by $I = 1/V$.

(i) Inner region, $x = O(\delta^{1/3})$

We write $x = \delta^{1/3} \hat{x}$, and in $\hat{x} = O(1)$ we pose

$$s \sim \hat{s}_0(\hat{x}, t), \quad i \sim \delta^{1/3} \hat{i}_0(\hat{x}, t), \quad p \sim \hat{s}_0(\hat{x}, t)/(1 - \lambda), \quad V \sim \delta^{-1/3} \hat{V}_0(\hat{x}, t)$$

to give

$$\hat{s}_0^3 = (1 - \lambda)^2 \hat{i}_0 \hat{V}_0, \quad \frac{\partial}{\partial \hat{x}} \left(\frac{\partial \hat{i}_0}{\partial \hat{x}} - \frac{\hat{i}_0}{\hat{s}_0} \frac{\partial \hat{s}_0}{\partial \hat{x}} \right) = 0, \quad \frac{\partial \hat{s}_0}{\partial t} = \beta \frac{\partial^2 \hat{V}_0}{\partial \hat{x}^2}. \quad (3.6)$$

Integrating the second equation of (3.6) once and matching into the outer region yields

$$\frac{\partial \hat{i}_0}{\partial \hat{x}} - \frac{\hat{i}_0}{\hat{s}_0} \frac{\partial \hat{s}_0}{\partial \hat{x}} = J(t) \quad (3.7)$$

where $J(t)$ is defined by (3.5); integrating (3.7) yields

$$\hat{i}_0 = J(t) \hat{s}_0(\hat{x}, t) \int_0^{\hat{x}} \frac{1}{\hat{s}_0(\mu, t)} d\mu, \quad \hat{V}_0 = \frac{\hat{s}_0^2(\hat{x}, t)}{J(t)(1 - \lambda)^2 \int_0^{\hat{x}} d\mu / \hat{s}_0(\mu, t)}. \quad (3.8)$$

We thus obtain a non-linear, non-local problem for $\hat{s}_0(\hat{x}, t)$ of a somewhat unusual form, namely,

$$\begin{aligned} \frac{\partial \hat{s}_0}{\partial t} &= \frac{\beta}{J(t)(1-\lambda)^2} \frac{\partial^2}{\partial \hat{x}^2} \left(\frac{\hat{s}_0^2}{\int_0^{\hat{x}} d\mu/\hat{s}_0(\mu, t)} \right), \\ \hat{s}_0 &\rightarrow 0 \quad \text{as } \hat{x} \rightarrow 0, \\ \hat{s}_0 &\rightarrow 1 \quad \text{as } \hat{x} \rightarrow +\infty, \\ \hat{s}_0 &= 1 \quad \text{at } t = 0. \end{aligned} \tag{3.9}$$

The leading order problem in $\hat{x} = O(1)$ is now completely specified. In order to discuss the next region, we introduce the positive quantity $L(t)$ defined by

$$L(t) \equiv \lim_{\hat{x} \rightarrow 0} \frac{\partial \hat{V}_0}{\partial \hat{x}};$$

this is determined by (3.9), the local behaviour being given as $\hat{x} \rightarrow 0$ by

$$\hat{s}_0 \sim (3JL(1-\lambda)^2 \hat{x}^2)^{1/3}, \quad \hat{i}_0 \sim 3J\hat{x}, \quad \hat{V}_0 \sim L\hat{x}. \tag{3.10}$$

The behaviour as $\hat{x} \rightarrow +\infty$ successfully matches with the outer solution. We note from (3.9) that

$$\frac{d}{dt} \int_0^\infty \hat{x}(\hat{s}_0(\hat{x}, t) - 1) d\hat{x} = \frac{\beta}{J(t)(1-\lambda)^2} \int_0^\infty \hat{x} \frac{\partial^2}{\partial \hat{x}^2} \left(\frac{\hat{s}_0^2}{\int_0^{\hat{x}} d\mu/\hat{s}_0(\mu, t)} \right) d\hat{x},$$

which yields zero upon integrating by parts. Hence

$$\int_0^\infty \hat{x}(\hat{s}_0(\hat{x}, t) - 1) d\hat{x} = 0.$$

so that \hat{s}_0 has a global maximum with $\hat{s}_0 > 1$ at some finite \hat{x}/\sqrt{t} (cf. Fig. 1); such a peak characterises dissociative-dominated behaviour and represents a type of uphill diffusion.

(ii) Inner inner region, $x = O(\delta^{2/3})$

We write $x = \delta^{2/3} x^*$ and

$$s \sim \delta^{2/3} s_0^*(x^*, t), \quad i \sim \delta^{2/3} i_0^*(x^*, t), \quad p \sim \delta^{2/3} s_0^*(x^*, t)/(1-\lambda), \quad V \sim V_0^*(x^*, t),$$

to obtain at leading order

$$s_0^{*3} = (1-\lambda)^2 i_0^* V_0^*, \quad \frac{\partial}{\partial x^*} \left(\frac{\partial i_0^*}{\partial x^*} - \frac{i_0^*}{s_0^*} \frac{\partial s_0^*}{\partial x^*} \right) = 0, \quad \frac{\partial^2 V_0^*}{\partial x^{*2}} = 0. \tag{3.11}$$

Integrating (3.11)₃ and matching yields

$$V_0^* = 1 + L(t)x^*.$$

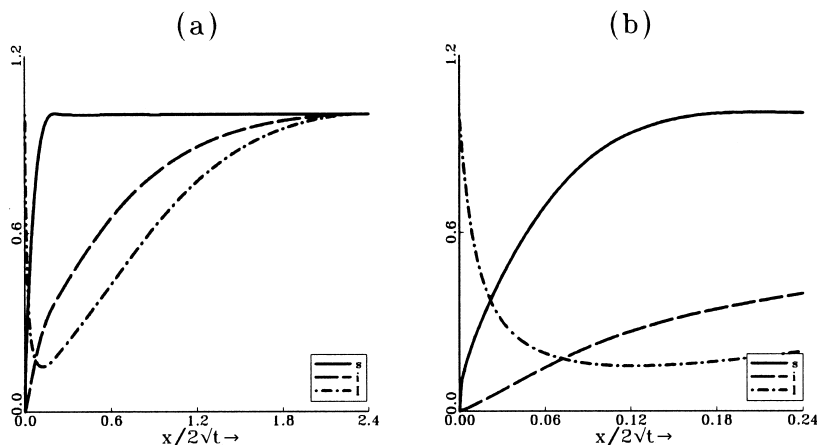


FIG. 1—A numerical solution of the dissociative model; the parameter values are $\delta = 0.001$, $\lambda = 0.4$, $\beta = 1$ and $\varpi = 0.0001$. (a) Full profiles; (b) magnification near the surface.

The remaining equations can also be readily integrated, and we obtain

$$s_0^* = \left(\frac{3J(1-\lambda)^2}{L} \right)^{\frac{1}{3}} (1 + Lx^*)^{1/2} ((1 + Lx^*)^{1/2} - 1)^{1/3},$$

$$i_0^* = \frac{3J}{L} (1 + Lx^*)^{1/2} ((1 + Lx^*)^{1/2} - 1). \tag{3.12}$$

This completes the analysis of the purely dissociative model. It is noteworthy that the leading order flux of impurity out of the semiconductor (given by $J(t)$) is controlled by the outer problem (3.3)–(3.4), whereas the flux of vacancies out (specified by $L(t)$) is dictated by the inner region. Excess vacancies are created by the out-diffusion of impurity; the surface acts as a sink for these, thereby removing a small proportion of them. As can be deduced from the I profile in Fig. 1 and from the asymptotics, a significant number of additional vacancies nevertheless remain in the bulk, with a corresponding depletion of self-interstitials. This is in sharp contrast to in-diffusion behaviour; see Part I.

3.3. Kick-out model

For $\delta = 0$, $\varepsilon \rightarrow 0$, three further regions in addition to the outer need to be considered. A numerical solution for this case is displayed in Fig. 2. We have $V = 1/I$.

(i) Surface region, $x = O(\varepsilon^{1/2})$

We write $x = \varepsilon^{\frac{1}{2}}x^*$ and

$$s \sim \varepsilon^{\frac{1}{6}}s_0^*(x^*, t), \quad i \sim \varepsilon^{\frac{1}{2}}i_0^*(x^*, t), \quad p \sim \varepsilon^{\frac{1}{6}}s_0^*(x^*, t)/(1-\lambda), \quad I \sim I_0^*(x^*, t),$$

to obtain the leading order equations

$$i_0^* = s_0^{*3} I_0^* / (1 - \lambda)^2, \quad \frac{\partial}{\partial x^*} \left(\frac{\partial i_0^*}{\partial x^*} - \frac{i_0^*}{s_0^*} \frac{\partial s_0^*}{\partial x^*} \right) = 0, \quad \frac{\partial^2 I_0^*}{\partial x^{*2}} = 0. \quad (3.13)$$

Integrating the second and third of these equations, we obtain

$$\frac{\partial i_0^*}{\partial x^*} - \frac{i_0^*}{s_0^*} \frac{\partial s_0^*}{\partial x^*} = J(t), \quad I_0^* = 1 - \frac{x^*}{q_0^*}, \quad (3.14)$$

where $J(t)$ is given by (3.5) and q_0^* gives the leading order location of a transition layer that will be determined later by matching. We now have

$$s_0^* = \frac{(q_0^* J (1 - \lambda)^2)^{1/3}}{(1 - x^*/q_0^*)^{1/2}} (1 - (1 - x^*/q_0^*)^{3/2})^{1/3},$$

$$i_0^* = \frac{q_0^{*3} J}{(1 - x^*/q_0^*)^{1/2}} (1 - (1 - x^*/q_0^*)^{3/2}). \quad (3.15)$$

The behaviour of these close to $x^* = q_0^*$ motivates the scaling in a transition between $x^* = O(1)$ and $x = O(1)$, which we discuss next. The somewhat unusual surface profile for s exhibited in Fig. 2(b) is in good agreement with the asymptotic result (3.15).

(ii) Interior layer

The transition layer is located at $z = O(1)$ where $x^* = q^*(t; \varepsilon) + \varepsilon^{1/3} z$, and in $z = O(1)$ we pose

$$s \sim s_0^\dagger(z, t), \quad i \sim \varepsilon^{1/3} i_0^\dagger(z, t), \quad p \sim s_0^\dagger(z, t) / (1 - \lambda), \quad I \sim \varepsilon^{1/3} I_0^\dagger(z, t),$$

to obtain at leading order

$$i_0^\dagger = s_0^{\dagger 3} I_0^\dagger / (1 - \lambda)^2, \quad \frac{\partial}{\partial z} \left(\frac{\partial i_0^\dagger}{\partial z} - \frac{i_0^\dagger}{s_0^\dagger} \frac{\partial s_0^\dagger}{\partial z} \right) = 0, \quad \dot{q}_0^* \frac{\partial s_0^\dagger}{\partial z} = \gamma \frac{\partial^2 I_0^\dagger}{\partial z^2}. \quad (3.16)$$

Integrating the third of these equations and matching forwards gives

$$-\dot{q}_0^* (1 - s_0^\dagger) = \gamma \frac{\partial I_0^\dagger}{\partial z}. \quad (3.17)$$

Using this equation to match with (3.14)–(3.15), we can easily show that

$$q_0^* = (2\gamma t)^{1/2}.$$

The second of (3.16) implies, matching with (3.15), that

$$i_0^\dagger = (q_0^* J / (1 - \lambda))^{2/3} s_0^{\dagger 3}, \quad (3.18)$$

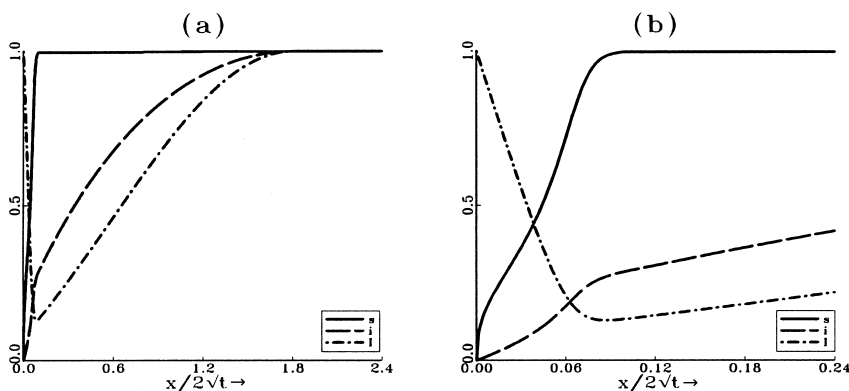


FIG. 2—A numerical solution of the kick-out model; the parameter values are $\varepsilon = 0.005$, $\lambda = 0.4$, $\gamma = 1$ and $\varpi = 0.0001$. (a) Full profiles; (b) magnification near the surface.

and (3.17) can then be written in separable form and integrated, since

$$s_0^{\ddagger 3} I_0^{\ddagger} = (q_0^* J (1 - \lambda)^2)^{2/3}.$$

As $z \rightarrow \infty$ we have

$$s_0^{\ddagger} \rightarrow 1, \quad i_0^{\ddagger} \rightarrow (q_0^* J / (1 - \lambda))^2, \quad I_0^{\ddagger} \rightarrow (q_0^* J (1 - \lambda)^2)^{2/3}. \quad (3.19)$$

(iii) Transition region, $x = O(\varepsilon^{1/3})$

The relevant scalings here are $x = \varepsilon^{1/3} x^{\ddagger}$ with

$$s \sim s_0^{\ddagger}(x^{\ddagger}, t), \quad i \sim \varepsilon^{1/3} i_0^{\ddagger}(x^{\ddagger}, t), \quad p \sim s_0^{\ddagger}(x^{\ddagger}, t) / (1 - \lambda), \quad I \sim \varepsilon^{1/3} I_0^{\ddagger}(x^{\ddagger}, t)$$

and

$$i_0^{\ddagger} = s_0^{\ddagger 3} I_0^{\ddagger} / (1 - \lambda)^2, \quad \frac{\partial}{\partial x^{\ddagger}} \left(\frac{\partial i_0^{\ddagger}}{\partial x^{\ddagger}} - \frac{i_0^{\ddagger}}{s_0^{\ddagger}} \frac{\partial s_0^{\ddagger}}{\partial x^{\ddagger}} \right) = 0, \quad \frac{\partial s_0^{\ddagger}}{\partial t} = 0, \quad (3.20)$$

so that

$$s_0^{\ddagger} = 1, \quad i_0^{\ddagger} = J x^{\ddagger} + (q_0^* J / (1 - \lambda))^2, \quad I_0^{\ddagger} = (1 - \lambda)^2 J x^{\ddagger} + (q_0^* J (1 - \lambda)^2)^{2/3}, \quad (3.21)$$

where we have matched backwards with (3.19) and forwards with (3.5).

This completes our asymptotic description of the kick-out case. Perhaps the main feature to note is the rather abrupt way in which s approaches 1; s increases rapidly in region (i) as x^* approaches q^* and then quickly levels off in the narrower region (ii). This behaviour is exhibited in Fig. 2(a) and may be contrasted with the smoother behaviour of Fig. 1. In Fig. 2(b) we give a magnification at the surface of the solutions displayed in Fig. 2(a). It is noteworthy that the increase in s is particularly rapid near $x = 0$, this behaviour also being evident from equation (3.15)₁, from

which we deduce that

$$s_0^* \sim \left(\frac{3}{2} J(1-\lambda)^2 x^* \right)^{1/3} \quad \text{as } x^* \rightarrow 0.$$

The kink in the profile for i in Fig. 2(a) corresponds to the rapid transition between the surface and outer regions that occurs over the interior layer described above. The numerical solution thus provides strong support for the asymptotic description just given.

3.4. Transition regimes

Numerical solutions illustrating some of the transition between dissociative and kick-out behaviour are displayed in Figs 3–4. To describe this transition asymptotically, we need to discuss two relations between ε and δ , the first of which is in some senses predominantly dissociative and the second predominantly kick-out.

(A) $\varepsilon = O(\delta^{5/6})$

We write $\varepsilon = a\delta^{5/6}$ where $a = O(1)$, and, in the limit $\delta \rightarrow 0$, the asymptotic structure comprises the following three regions in addition to the outer.

(i) Surface region, $x = O(\delta^{1/2})$

Here we write $x = \delta^{1/2}x^*$, the appropriate scalings being

$$s \sim \delta^{1/6}s_0^*(x^*, t), \quad i \sim \delta^{1/2}i_0^*(x^*, t), \quad p \sim \delta^{1/6}s_0^*/(1-\lambda), \quad I \sim I_0^*(x^*, t), \quad V \sim V_0^*(x^*, t),$$

to give from (1.2) the leading order balance (3.13) with $V_0^* = 1/I_0^*$, with solution given by (3.15) and

$$I_0^* = 1 - x^*/q_0^*, \quad V_0^* = 1/(1 - x^*/q_0^*), \quad (3.22)$$

where q_0^* (the location of an interior layer, whose structure we discuss next) again remains to be determined.

(ii) Interior layer

Here we write $x^* = q^*(t; \delta) + \delta^{1/12}z$, the appropriate scalings for $z = O(1)$ being given by $q^* \sim q_0^*(t)$ with

$$s \sim \delta^{1/8}s_0^\dagger(z, t), \quad i \sim \delta^{11/24}i_0^\dagger(z, t), \quad p \sim \delta^{1/8}s_0^\dagger/(1-\lambda), \\ I \sim \delta^{1/12}I_0^\dagger(z, t), \quad V \sim \delta^{-1/12}V_0^\dagger(z, t),$$

and the leading order balance by

$$i_0^\dagger = I_0^\dagger s_0^{\dagger 3}/(1-\lambda)^2, \quad I_0^\dagger V_0^\dagger = 1, \\ \frac{\partial}{\partial z} \left(\frac{\partial i_0^\dagger}{\partial z} - \frac{i_0^\dagger}{s_0^\dagger} \frac{\partial s_0^\dagger}{\partial z} \right) = 0, \quad \beta \frac{\partial^2 V_0^\dagger}{\partial z^2} - \gamma a \frac{\partial^2 I_0^\dagger}{\partial z^2} = 0.$$

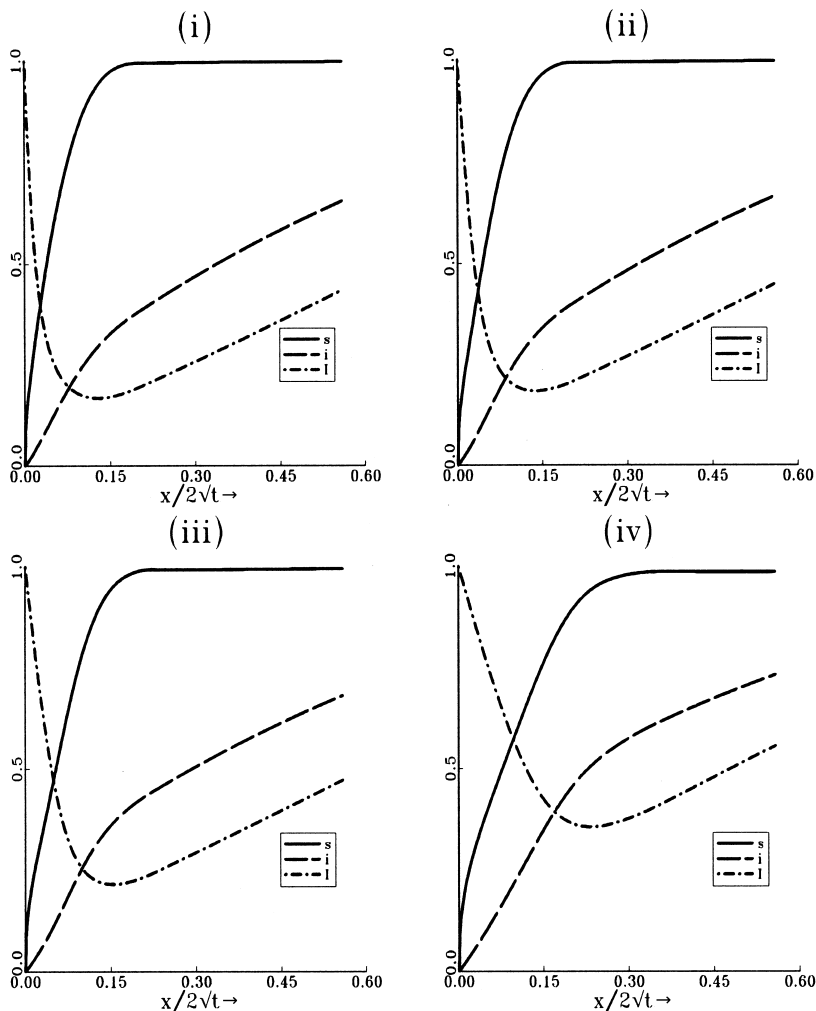


FIG. 3—Magnification near the surface of numerical solutions for the defect neutral model. The parameter values are $\beta = \gamma = 1$, $\lambda = 0.4$, $\delta = 0.001$, $\varpi = 0.0001$ and (i) $\varepsilon = 0.001$, (ii) $\varepsilon = 0.003$, (iii) $\varepsilon = 0.007$ and (iv) $\varepsilon = 0.03$. The progression is from dissociative to kick-out domination.

The diffusion terms for V and I thus both enter at leading order in this region. Matching with (3.22), we have

$$i_0^\dagger = (q_0^* J / (1 - \lambda))^{2/3} s_0^\dagger, \quad \beta V_0^\dagger - \gamma a I_0^\dagger = \gamma a z / q_0^*, \quad (3.23)$$

it being convenient to define $q^*(t; \delta)$ to all orders via

$$\beta \delta V - \gamma \varepsilon I = 0 \quad \text{at} \quad x^* = q^*.$$

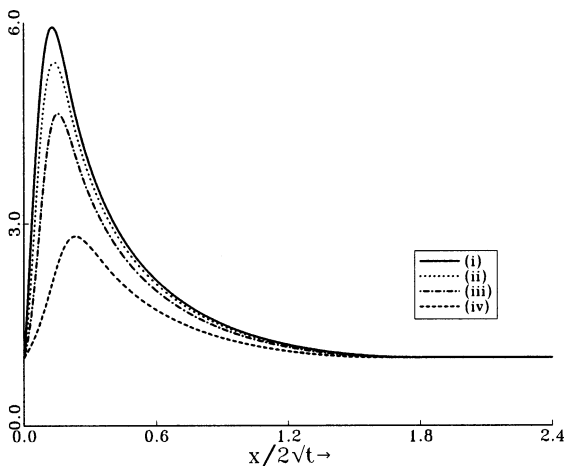


FIG. 4—Numerically calculated vacancy profiles of the defect neutral model, illustrating the vacancy supersaturation. The parameter values used can be found in the caption for Fig. 3.

Hence

$$V_0^\dagger = \frac{\gamma a}{2\beta q_0^*} ((z^2 + 4\beta q_0^*/\gamma a)^{1/2} + z), \quad I_0^\dagger = \frac{1}{2q_0^*} ((z^2 + 4\beta q_0^*/\gamma a)^{1/2} - z), \quad (3.24)$$

with

$$s_0^\dagger = (q_0^* J (1 - \lambda)^2)^{1/3} V_0^{\dagger 1/2}. \quad (3.25)$$

(iii) Inner region, $x = O(\delta^{1/3})$

This inner region is closely related to that discussed in Section 2.2. We again write $x = \delta^{1/3} \hat{x}$ and pose

$$s \sim \hat{s}_0(\hat{x}, t), \quad i \sim \delta^{1/3} \hat{i}_0(\hat{x}, t), \quad p \sim \hat{s}_0/(1 - \lambda), \quad I \sim \delta^{1/3} \hat{I}_0(\hat{x}, t), \quad V \sim \delta^{-1/3} \hat{V}_0(\hat{x}, t)$$

to obtain at leading order

$$\begin{aligned} \hat{s}_0^3/(1 - \lambda)^2 &= \hat{i}_0 \hat{V}_0, & \hat{I}_0 \hat{V}_0 &= 1, \\ \frac{\partial \hat{i}_0}{\partial \hat{x}} - \frac{\hat{i}_0}{\hat{s}_0} \frac{\partial \hat{s}_0}{\partial \hat{x}} &= J(t), & \frac{\partial \hat{s}_0}{\partial t} &= \beta \frac{\partial^2 \hat{V}_0}{\partial \hat{x}^2}. \end{aligned} \quad (3.26)$$

In view of (3.23), we now have

$$\hat{i}_0 = (q_0^* J / (1 - \lambda))^2 \hat{s}_0 + J \hat{s}_0 \int_0^{\hat{x}} \frac{1}{\hat{s}_0(\mu, t)} d\mu, \quad (3.27)$$

cf. (3.8), and we may again formulate the problem as a single (non-local) equation for \hat{s}_0 . The boundary and initial conditions are the same as those in (3.9), but (3.10)

is replaced by

$$\hat{s}_0 \sim (q_0^* J(1-\lambda)^2)^{1/3} L^{1/2} \hat{x}^{1/2}, \quad \hat{i}_0 \sim q_0^* J L^{1/2} \hat{x}^{1/2}, \quad \hat{V}_0 \sim L \hat{x} \quad \text{as } \hat{x} \rightarrow 0. \quad (3.28)$$

Matching with (3.24) can now be accomplished, determining q_0^* via

$$q_0^* = \gamma a / \beta L; \quad (3.29)$$

substituting this into (3.27)–(3.28) leads to a correctly specified leading order problem in $\hat{x} = O(1)$ in which $L(t)$ is determined as part of the solution. The transition layer location is then fixed by (3.29). In the limit $a \rightarrow 0$ it follows that (3.27) reduces to (3.8), and we recover the purely dissociative inner region; the significance of the transition scaling $\varepsilon = O(\delta^{5/6})$ follows from the changes that occur in the inner region over this scaling. The region can be regarded as dissociative-dominated, although kick-out effects enter through the behaviour as $\hat{x} \rightarrow 0$.

As $\hat{x} \rightarrow +\infty$ we again have

$$\hat{s}_0 \rightarrow 1, \quad \hat{i}_0 \sim J(t)\hat{x}, \quad \hat{V}_0 \sim 1/(1-\lambda)^2 J(t)\hat{x},$$

matching into the outer region.

(B) $\varepsilon = O(\delta^{3/4})$

We write $\varepsilon = b\delta^{3/4}$ where $b = O(1)$, and, in the limit $\delta \rightarrow 0$, the asymptotic structure is as follows.

(i) Surface region, $x = O(\delta^{3/8})$

We write $x = \delta^{3/8} x^*$ with $0 < x^* < q_0^*(t)$ and with scalings

$$s \sim \delta^{1/8} s_0^*(x^*, t), \quad i \sim \delta^{3/8} i_0^*(x^*, t), \quad p \sim \delta^{1/8} s_0^*/(1-\lambda), \quad I \sim I_0^*(x^*, t), \quad V \sim V_0^*(x^*, t).$$

The leading order equations are as in (A), with the solution in $x^* < q_0^*(t)$ being given by (3.15) and (3.22).

(ii) Interior layer

We define z by $x^* = q_0^*(t; \delta) + \delta^{1/8} z$ and write

$$s \sim \delta^{1/16} s_0^\dagger(z, t), \quad i \sim \delta^{5/16} i_0^\dagger(z, t), \quad p \sim \delta^{1/16} s_0^\dagger/(1-\lambda), \\ I \sim \delta^{1/8} I_0^\dagger(z, t), \quad V \sim \delta^{-1/8} V_0^\dagger(z, t),$$

and recover the same leading order solution (3.23)–(3.25) as in case (A), except that a is replaced by b .

(iii) Inner region, $x = O(\delta^{3/8})$

The x scaling, $x = \delta^{3/8} x^*$, is the same as in region (i), but the analysis now holds in $x^* > q_0^*(t)$. The scalings are

$$s \sim \hat{s}_0(x^*, t), \quad i \sim \delta^{1/4} \hat{i}_0(x^*, t), \quad p \sim \hat{s}_0/(1-\lambda), \quad I \sim \delta^{1/4} \hat{I}_0(x^*, t), \quad V \sim \delta^{-1/4} \hat{V}_0(x^*, t),$$

which give, via matching with (ii),

$$\hat{i}_0 = (q_0^* J / (1 - \lambda))^2 / 3 \hat{s}_0, \quad \hat{V}_0 = \hat{s}_0^2 / (q_0^* J (1 - \lambda)^2)^{2/3}$$

and the moving boundary problem

$$\begin{aligned} \frac{\partial \hat{s}_0}{\partial t} &= \frac{2\beta}{(q_0^* J (1 - \lambda)^2)^{2/3}} \frac{\partial}{\partial x^*} \left(\hat{s}_0 \frac{\partial \hat{s}_0}{\partial x^*} \right), \\ \hat{s}_0 \rightarrow 0, \quad \frac{2\beta}{(J(1 - \lambda)^2)^{2/3}} \hat{s}_0 \frac{\partial \hat{s}_0}{\partial x^*} &= \frac{\gamma b}{q_0^{*1/3}} \quad \text{as } x^* \rightarrow q_0^{*+}, \\ \hat{s}_0 \rightarrow 1 \quad \text{as } x^* \rightarrow +\infty, \\ q_0^* &= 0 \quad \text{at } t = 0, \end{aligned} \tag{3.30}$$

which determines q_0^* as well as \hat{s}_0 . Kick-out effects thus enter again through the b dependence of the moving boundary condition; that they do so in this leading order fashion identifies $\varepsilon = O(\delta^{3/4})$ as the second transition scaling. If we compare the analysis with case (A), the partial differential equation in (3.30) corresponds to the non-local term in (3.27) being negligible; the dependence of the second moving boundary condition in (3.30) on $q_0^{*1/3}$ provides a novelty of the current formulation. Since $q_0^* J$ is constant in the current (self-similar) context, writing

$$\hat{x} = \frac{(2\beta)^{1/2}}{(q_0^* J (1 - \lambda)^2)^{1/3}} \hat{X}$$

leads to a form in which the diffusivity does not depend on the unknown q_0^* , and scaling arguments can be used to show that $q_0^* / b^{3/2} \rightarrow \text{constant}$ as $b \rightarrow 0$.

(iv) Transition region, $x = O(\delta^{1/4})$

We write $x = \delta^{1/4} x^\ddagger$, and in $x^\ddagger = O(1)$ we have

$$s \sim s_0^\ddagger(x^\ddagger, t), \quad i \sim \delta^{1/4} i_0^\ddagger(x^\ddagger, t), \quad p \sim s_0^\ddagger / (1 - \lambda), \quad I \sim \delta^{1/4} I_0^\ddagger(x^\ddagger, t), \quad V \sim \delta^{-1/4} V_0^\ddagger(x^\ddagger, t)$$

and we recover (3.20)–(3.21).

This completes our analysis of the two regimes that give the transition from pure dissociative to pure kick-out behaviour; we defer discussion of the results to Section 5.

4. The charged defect model

4.1. Outer region, $x = O(1)$

In this subsection we consider the solutions to equations (1.4) subject to the boundary and initial conditions (1.3) and discuss the dissociative and kick-out cases, together with a single transition scaling. However, the analysis in the outer region is identical for all three cases, and we give this first. We again set $\varpi = 0$ throughout, simplifying

the charge neutrality condition in (1.4) to

$$p = (s - \lambda i - 2\epsilon I)/(1 - \lambda - 2\epsilon);$$

the ϵ terms in this expression will prove to be negligible throughout what follows.

All concentrations are $O(1)$ in $x = O(1)$, and we pose

$$s \sim s_0(x, t), \quad i \sim i_0(x, t), \quad p \sim p_0(x, t), \quad I \sim I_0(x, t), \quad V \sim V_0(x, t)$$

to obtain at leading order (the analysis being very close to that of Section 3.1)

$$s_0 = 1, \quad p_0 = (1 - \lambda i_0)/(1 - \lambda), \quad I_0 = i_0, \quad V_0 = (1 - \lambda i_0)^2/(1 - \lambda)^2 i_0$$

where i_0 is determined by solving (3.3)–(3.4). It is worth noting that neither self-interstitial nor vacancy diffusion plays a role in the outer region. We have as matching conditions that

$$p_0 \sim 1/(1 - \lambda), \quad i_0 = I_0 \sim J(t)x, \quad V_0 \sim 1/(1 - \lambda)^2 J(t)x \quad \text{as } x \rightarrow 0^+ \quad (4.1)$$

where $J(t)$ is defined by (3.5). It is worth remembering that, since the problem is self-similar, we have $J(t) = J_0/\sqrt{t}$ where J_0 is a constant. For the remainder of the asymptotic analysis, we need to distinguish between the different cases.

4.2. Dissociative model

When $\epsilon = 0$ the problem is identical to that discussed in Section 3.2, although I is now given by $I = p^2/V$; however, as we shall see, case (II) behaves significantly differently from case (I) when kick-out effects are included.

4.3. Kick-out model

For $\delta = 0$, there are three further regions to be considered in addition to the outer. V decouples, being given by $V = p^2/I$.

A numerical solution for the charged defect kick-out model can be found in Fig. 5.

(i) Surface region, $x = O((\epsilon/\ln(1/\epsilon))^{3/4})$

We write $x = (\epsilon/\ln(1/\epsilon))^{3/4} x^*$ and

$$\begin{aligned} s &\sim (\epsilon/\ln(1/\epsilon))^{1/4} s_0^*(x^*, t), & i &\sim (\epsilon/\ln(1/\epsilon))^{3/4} i_0^*(x^*, t), \\ p &\sim (\epsilon/\ln(1/\epsilon))^{1/4} s_0^*/(1 - \lambda), & I &\sim (\epsilon/\ln(1/\epsilon))^{1/2} I_0^*(x^*, t); \end{aligned}$$

these scalings are required for matching into region (ii) below. The leading order equations yield

$$i_0^* = s_0^* I_0^*, \quad s_0^* \frac{\partial I_0^*}{\partial x^*} = J(t), \quad \frac{\partial I_0^*}{\partial x^*} - \frac{2I_0^*}{s_0^*} \frac{\partial s_0^*}{\partial x^*} = -M(t), \quad (4.2)$$

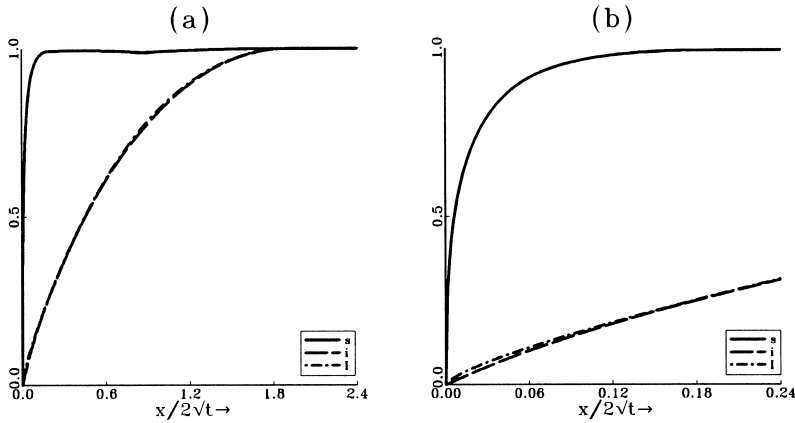


FIG. 5—Numerical solution of the charged defect kick-out model. The parameter values are $\gamma = 1$, $\lambda = 0.4$, $\varepsilon = 0.05$ and $\varpi = 0.0001$. (a) Full profiles; (b) magnification near the surface.

where $M(t)$ will be determined below. From these we may obtain

$$s_0^* = (1 - \lambda)I_0^{*\frac{1}{2}} / (1 - M(1 - \lambda)I_0^{*\frac{1}{2}}/J),$$

$$\frac{1}{M}I_0^* + \frac{2J}{M^2(1 - \lambda)}I_0^{*\frac{1}{2}} + \frac{2J^2}{M^3(1 - \lambda)^2} \ln(1 - M(1 - \lambda)I_0^{*\frac{1}{2}}/J) = -x^*, \quad (4.3)$$

so as $x^* \rightarrow +\infty$

$$I_0^* \sim \frac{J^2}{M^2(1 - \lambda)^2}, \quad s_0^* \sim \frac{J}{M} e^3 e^{M^3(1-\lambda)^2 x^*/2J^2}. \quad (4.4)$$

This represents less abrupt growth of s than in the neutral defect case (cf. (3.15)).

(ii) Interior layer

There is an interior layer located at $z = O(1)$ where $x^* = q(t; \varepsilon) \ln(1/\varepsilon) + z$, with scalings

$$s \sim s_0^\dagger(z, t), \quad i \sim (\varepsilon/\ln(1/\varepsilon))^{\frac{1}{2}} i_0^\dagger(z, t), \quad p \sim s_0^\dagger/(1 - \lambda), \quad I \sim (\varepsilon/\ln(1/\varepsilon))^{\frac{1}{2}} I_0^\dagger(z, t).$$

The leading order equations can be written

$$i_0^\dagger = s_0^\dagger I_0^\dagger, \quad \frac{\partial I_0^\dagger}{\partial z} = 0, \quad -\dot{q}_0 \frac{\partial s_0^\dagger}{\partial z} = \gamma \frac{\partial}{\partial z} \left(\frac{\partial I_0^\dagger}{\partial z} - \frac{2I_0^\dagger}{s_0^\dagger} \frac{\partial s_0^\dagger}{\partial z} \right), \quad (4.5)$$

where

$$q(t; \delta) \sim q_0(t) = J^2/2M^3(1 - \lambda)^2 \quad (4.6)$$

follows by matching with (4.4), which gives additionally that

$$I_0^\dagger = J^2/M^2(1 - \lambda)^2$$

and

$$\dot{q}_0(1 - s_0^\dagger) = \frac{2\gamma J^2}{M^2(1 - \lambda)^2} \frac{1}{s_0^\dagger} \frac{\partial s_0^\dagger}{\partial z} \quad (4.7)$$

where we have also matched with the outer region. The conditions (4.4) now require further that

$$\dot{q}_0 = \gamma M,$$

which, together with (4.6), gives

$$q_0 = \gamma^{\frac{3}{4}} \left(\frac{2J_0}{(1 - \lambda)} \right)^{\frac{1}{2}} t^{\frac{1}{2}}, \quad M = \gamma^{-\frac{1}{4}} \left(\frac{J_0}{2(1 - \lambda)} \right)^{\frac{1}{2}} t^{-\frac{1}{2}}.$$

This interior layer separates the regions in which $s \sim 1$ from the surface region, in which $s \ll 1$.

(iii) Transition region, $x = O((\varepsilon/\ln(1/\varepsilon))^{1/2})$

Taking $x = (\varepsilon/\ln(1/\varepsilon))^{1/2} x^\ddagger$, we obtain similar behaviour to that described in Section 3.3(iii), with

$$s \sim 1, \quad p \sim 1/(1 - \lambda), \quad i, I \sim (\varepsilon/\ln(1/\varepsilon))^{1/2} (Jx^\ddagger + J^2/M^2(1 - \lambda))^2,$$

completing the matching with the outer region.

4.4. Transition scalings

Introduction. We mention three different scalings through which the transition between the two mechanisms occurs. For $\varepsilon = O(\delta^{5/9})$ the terms in γ influence the inner inner region of Section 3.2, entering the final equation of (3.11), but the behaviour is largely dissociative-dominated, with the leading order inner solution being as in Section 3.2. The most significant regime for the transition, and the only one we discuss in detail, has $\varepsilon = b\delta^{\frac{1}{2}}$ with $b = O(1)$; we must treat separately the cases $b < b_c$ and $b > b_c$, where b_c is defined below. Numerical solutions for various values of b can be found in Fig. 6. The final regime is $\varepsilon = O(\delta^{\frac{1}{2}} \ln^{\frac{1}{2}}(1/\delta))$, about which we restrict ourselves to the comment that this scaling makes possible the description of the transition to purely kick-out behaviour via the introduction of the term $\beta \partial V_0^\dagger / \partial z$ into the last equation of (4.5).

The case $b < b_c$. There are three further regions to discuss in addition to the outer.

(i) Surface region, $x = O(\delta^{1/2})$

We write $x = \delta^{\frac{1}{2}} x^*$, and in $x^* = O(1)$ we pose

$$s \sim \delta^{\frac{1}{6}} s_0^*(x^*, t), \quad i \sim \delta^{\frac{1}{2}} i_0^*(x^*, t), \quad p \sim \delta^{\frac{1}{6}} s_0^*/(1 - \lambda), \quad I \sim \delta^{\frac{1}{3}} I_0^*(x^*, t), \quad V \sim V_0^*(x^*, t),$$

to recover the leading order equations (4.2)–(4.4), with $I_0^* V_0^* = s_0^{*2}/(1 - \lambda)^2$; the quantity $M(t)$ depends on b through the problem described in (iii) below.

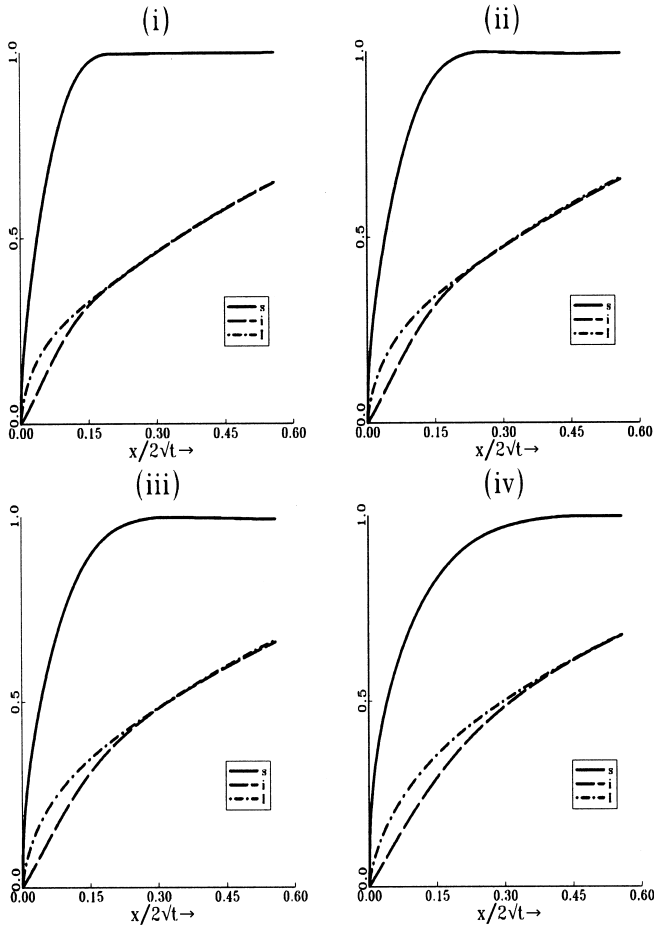


FIG. 6—Magnification near the surface of numerical solutions for the charged defect model. The parameter values are $\beta = \gamma = 1$, $\lambda = 0.4$, $\delta = 0.001$, $\varpi = 0.0001$ and (i) $b = 0.05$, (ii) $b = 0.5$, (iii) $b = 1.0$ and (iv) $b = 3.0$.

(ii) Interior layer

This is located at $z = O(1)$ where $x^* = q(t; \delta) \ln(1/\delta) + z$ and where the appropriate scalings are given by

$$s \sim \delta^{\frac{1}{12}} s_0^\dagger(z, t), \quad i \sim \delta^{\frac{5}{12}} i_0^\dagger(z, t), \quad p \sim \delta^{\frac{1}{12}} s_0^\dagger / (1 - \lambda), \quad I \sim \delta^{\frac{1}{3}} I_0^\dagger(z, t), \quad V \sim \delta^{-\frac{1}{6}} V_0^\dagger(z, t)$$

with

$$q(t; \delta) \sim q_0(t) = J^2 / 6M^3 (1 - \lambda)^2. \tag{4.8}$$

We have

$$I_0^\dagger = J^2 / M^2 (1 - \lambda)^2, \quad V_0^\dagger = M^2 s_0^{\dagger 2} / J^2, \quad i_0^\dagger = J^2 s_0^\dagger / M^2 (1 - \lambda)^2 \tag{4.9}$$

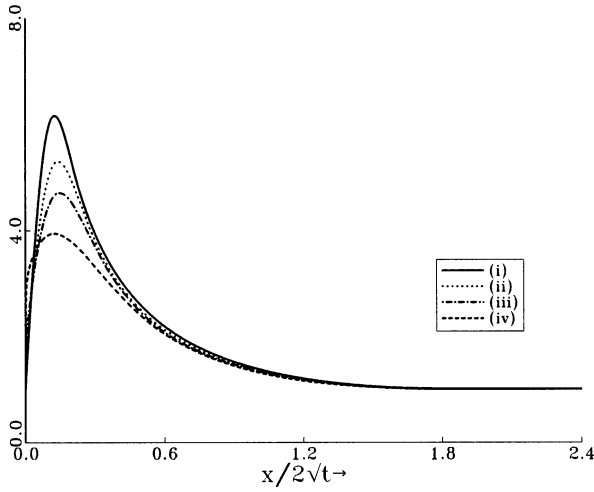


FIG. 7—Numerically calculated vacancy profiles of the charged defect model, illustrating vacancy supersaturation. The parameter values used can be found in the caption for Fig. 6.

and

$$\beta \frac{\partial V_0^\dagger}{\partial z} + \frac{2\gamma b J^2}{M^2(1-\lambda)^2} \frac{1}{s_0^\dagger} \frac{\partial s_0^\dagger}{\partial z} = \gamma b M,$$

so that

$$\beta \frac{M^2}{J^2} s_0^{\dagger 2} + \frac{2\gamma b J^2}{M^2(1-\lambda)^2} \ln s_0^\dagger = \gamma b M z. \quad (4.10)$$

While region (i) is of purely kick-out form, dissociative effects are significant (through the β term) in (4.10); in particular, we have

$$s_0^\dagger \sim J(\gamma b / \beta M)^{1/2} z^{1/2} \quad \text{as } z \rightarrow +\infty.$$

We note more generally that kick-out effects tend to be strongest near $x = 0$, since the surface acts as a sink for the supersaturation of vacancies generated in the bulk; see Fig. 7.

(iii) Inner region, $x = O(\delta^{1/3})$

The scalings of Section 3.2(i) are recovered (with $I \sim \delta^{1/3} \hat{I}_0(\hat{x}, t)$), along with (3.6) and $\hat{s}_0 \hat{I}_0 = \hat{i}_0$, but the boundary conditions are replaced by

$$\begin{aligned} \hat{V}_0 &= 0, & \frac{\partial \hat{V}_0}{\partial \hat{x}} &= \frac{\gamma b M}{\beta}, & \hat{I}_0 &= \frac{J^2}{M^2(1-\lambda)^2} & \text{on } \hat{x} = 0, \\ \hat{s}_0 &\rightarrow 1 & \text{as } \hat{x} &\rightarrow +\infty, \\ \hat{s}_0 &= 1 & \text{at } t &= 0, \end{aligned} \quad (4.11)$$

where we have matched into the interior layer; this change in the boundary conditions for \hat{I}_0 is one of the means of identifying $\varepsilon = O(\delta^{\frac{1}{2}})$ as an important transition regime. The problem may again be formulated as a novel type of non-local diffusion problem for \hat{s}_0 . In place of (3.10) and in view of (4.11)₁, we have as $\hat{x} \rightarrow 0$ that

$$\hat{V}_0 \sim \frac{\gamma b M \hat{x}}{\beta}, \quad \hat{I}_0 \sim \frac{J^2}{M^2(1-\lambda)^2},$$

and then, using $\hat{s}_0 \hat{I}_0 = \hat{i}_0$ and $\hat{s}_0^3 = (1-\lambda)^2 \hat{i}_0 \hat{V}_0$, it follows that

$$\hat{s}_0 \sim J \left(\frac{\gamma b}{\beta M} \right)^{\frac{1}{2}} \hat{x}^{\frac{1}{2}}, \quad \hat{i}_0 \sim \frac{J^3}{M^2(1-\lambda)^2} \left(\frac{\gamma b}{\beta M} \right)^{\frac{1}{2}} \hat{x}^{\frac{1}{2}} \quad \text{as } \hat{x} \rightarrow 0,$$

M being determined as part of the solution to (3.6) and (4.11); as we shall now see, it is a sensitive function of b .

Accordingly, we now analyse (3.6) and (4.11) in the limit $M \rightarrow 0$, showing that this occurs at a finite value (b_c) of b . We first make the rescaling $\hat{x} = (2\beta)^{\frac{1}{2}} M \hat{X} / J$, noting that M/J is constant since self-similarity implies that $J(t)$ and $M(t)$ have the form $J(t) = J_0/\sqrt{t}$, $M(t) = M_0/\sqrt{t}$ with J_0, M_0 constants. Letting $M_0 \rightarrow 0$ with $\hat{X} = O(1)$ in the second equation of (3.6) gives

$$\frac{\partial \hat{i}_0}{\partial \hat{X}} \sim \frac{\hat{i}_0}{\hat{s}_0} \frac{\partial \hat{s}_0}{\partial \hat{X}},$$

so integrating and matching with the third equation of (4.9) yields

$$\hat{i}_0 \sim J^2 \hat{s}_0 / M^2 (1-\lambda)^2,$$

from which it follows that

$$\hat{I}_0 \sim J^2 / M^2 (1-\lambda)^2, \quad \hat{V}_0 \sim M^2 \hat{s}_0^2 / J^2.$$

Writing $\hat{s}_0 \sim \hat{S}(\hat{X}, t)$ as $M_0 \rightarrow 0$ with $\hat{X} = O(1)$ now gives

$$\begin{aligned} \frac{\partial \hat{S}}{\partial t} &= \frac{\partial}{\partial \hat{X}} \left(\hat{S} \frac{\partial \hat{S}}{\partial \hat{X}} \right), \\ \hat{S} \rightarrow 0, \quad \hat{S} \frac{\partial \hat{S}}{\partial \hat{X}} &\rightarrow \frac{\gamma b J}{(2\beta)^{\frac{1}{2}}} \quad \text{as } \hat{X} \rightarrow 0^+, \\ \hat{S} &\rightarrow 1 \quad \text{as } \hat{X} \rightarrow +\infty, \\ \hat{S} &= 1 \quad \text{at } t = 0. \end{aligned} \tag{4.12}$$

The solution to (4.12) is determined uniquely without imposing the second condition on $\hat{X} = 0$, which thus serves to determine b_c via

$$b_c = \frac{(2\beta)^{\frac{1}{2}}}{\gamma J} \lim_{\hat{X} \rightarrow 0^+} \hat{S} \frac{\partial \hat{S}}{\partial \hat{X}}. \tag{4.13}$$

Solving (3.3) subject to (3.4) numerically for $\lambda = 0.4$ (which is the value for λ that has been used throughout the numerical work of this paper), we obtain the estimate $J(t) \approx 0.62/\sqrt{t}$ and we find by solving (4.12) numerically that

$$\lim_{\hat{x} \rightarrow 0^+} \hat{S} \frac{\partial \hat{S}}{\partial \hat{X}} \approx \frac{0.33}{\sqrt{t}},$$

so for $\lambda = 0.4$ we have $b_c \approx (2\beta)^{1/2} 0.53/\gamma$; for the numerical work of this paper we use $\beta = \gamma = 1$, so this becomes $b_c \approx 0.75$.

We note from (4.8) that $q_0 \rightarrow +\infty$ as $M \rightarrow 0$, which provides an indication of the behaviour to be expected for $b > b_c$. The above formulation applies for sufficiently small b , but M decreases as b is increased, dropping to zero at a finite value $b = b_c$ (given by (4.13)); a different formulation of the problem is thus required for $b > b_c$, which we now describe.

The case $b > b_c$: moving boundary problem. There are four further regions in this case, the third being the most significant.

(i) Surface region, $x = O(\delta^{3/8} \ln^{-3/4}(1/\delta))$

We write $x = \delta^{3/8} \ln^{-3/4}(1/\delta)x^*$ and

$$\begin{aligned} s &\sim \delta^{1/8} \ln^{-1/4}(1/\delta)s_0^*(x^*, t), & i &\sim \delta^{3/8} \ln^{-3/4}(1/\delta)i_0^*(x^*, t), \\ p &\sim \delta^{1/8} \ln^{-1/4}(1/\delta)s_0^*/(1-\lambda), & I &\sim \delta^{1/4} \ln^{-1/2}(1/\delta)I_0^*(x^*, t), & V &\sim V_0^*(x^*, t), \end{aligned}$$

again giving (4.2)–(4.4) with $I_0^*V_0^* = s_0^{*2}/(1-\lambda)$.

(ii) Interior layer

This region is at $z = O(1)$ where $x^* = q(t; \delta) \ln(1/\delta) + z$, and we write

$$\begin{aligned} s &\sim \ln^{-1/2}(1/\delta)s_0^\dagger(z, t), & i &\sim \delta^{1/4} \ln^{-1}(1/\delta)i_0^\dagger(z, t), & p &\sim \ln^{-1/2}(1/\delta)s_0^\dagger/(1-\lambda), \\ I &\sim \delta^{1/4} \ln^{-1/2}(1/\delta)I_0^\dagger(z, t), & V &\sim \delta^{-1/4} \ln^{-1/2}(1/\delta)V_0^\dagger(z, t), \end{aligned}$$

with

$$q_0 = J^2/4M^3(1-\lambda)^2, \tag{4.14}$$

giving (4.9)–(4.10).

(iii) Inner region, $x = O(\delta^{3/8} \ln^{1/4}(1/\delta))$

We write $x = \delta^{3/8} \ln^{1/4}(1/\delta)\hat{x}$ and

$$\begin{aligned} s &\sim \hat{s}_0(\hat{x}, t), & i &\sim \delta^{1/4} \ln^{-1/2}(1/\delta)\hat{i}_0(\hat{x}, t), & p &\sim \hat{s}_0/(1-\lambda), & I &\sim \delta^{1/4} \ln^{-1/2}(1/\delta)\hat{I}_0(\hat{x}, t), \\ V &\sim \delta^{-1/4} \ln^{1/2}(1/\delta)\hat{V}_0(\hat{x}, t), \end{aligned}$$

with leading order equations

$$\begin{aligned}\hat{s}_0 &= (1 - \lambda)^2 \hat{i}_0 \hat{V}_0, & \hat{s}_0 \hat{I}_0 &= \hat{i}_0, \\ \frac{\partial}{\partial \hat{x}} \left(\frac{\partial \hat{i}_0}{\partial \hat{x}} - \frac{\hat{i}_0}{\hat{s}_0} \frac{\partial \hat{s}_0}{\partial \hat{x}} \right) &= 0, & \frac{\partial \hat{s}_0}{\partial t} &= \beta \frac{\partial^2 \hat{V}_0}{\partial \hat{x}^2},\end{aligned}$$

from which it follows, on matching with (4.9), that

$$\hat{i}_0 = J^2 \hat{s}_0 / M^2 (1 - \lambda)^2, \quad \hat{I}_0 = J^2 / M^2 (1 - \lambda)^2, \quad \hat{V}_0 = M^2 \hat{s}_0^2 / J^2,$$

and, writing $\hat{x} = (2\beta)^{\frac{1}{2}} M \hat{X} / J$, $q_0 = (2\beta)^{1/2} M Q_0 / J$,

$$\begin{aligned}\frac{\partial \hat{s}_0}{\partial t} &= \frac{\partial}{\partial \hat{X}} \left(\hat{s}_0 \frac{\partial \hat{s}_0}{\partial \hat{X}} \right), \\ \hat{s}_0 &\rightarrow 0, \quad \hat{s}_0 \frac{\partial \hat{s}_0}{\partial \hat{X}} \rightarrow \gamma b J / (2\beta)^{\frac{1}{2}} \quad \text{as } \hat{X} \rightarrow Q_0(t)^+, \\ \hat{s}_0 &\rightarrow 1 \quad \text{as } \hat{X} \rightarrow +\infty, \\ \hat{s}_0 &= 1 \quad \text{at } t = 0,\end{aligned}\tag{4.15}$$

where, in view of (4.14), the moving boundary location satisfies

$$Q_0(t) = J^3 / 4M^4 (1 - \lambda)^2 (2\beta)^{\frac{1}{2}};\tag{4.16}$$

it is to be found as part of the solution to (4.15), thereby determining M via (4.16). We thus have a problem for the porous medium equation in which material is extracted at a specified rate at the moving boundary (by substitutional impurity becoming interstitial). We note by comparison with (4.12) that $Q_0 \rightarrow 0^+$ (and hence $M \rightarrow \infty$) as $b \rightarrow b_c^+$, as expected in view of the analysis above.

(iv) Transition region, $x = O(\delta^{1/4} \ln^{-1/2}(1/\delta))$

We write $x = \delta^{\frac{1}{4}} \ln^{-\frac{1}{2}}(1/\delta) x^\ddagger$, the structure being very similar to previous transition layers, with

$$\begin{aligned}s &\sim 1, \quad p \sim 1/(1 - \lambda), \\ i, I &\sim \delta^{\frac{1}{4}} \ln^{-\frac{1}{2}}(1/\delta) (J x^\ddagger + J^2 / (1 - \lambda)^2 M^2), \\ V &\sim \delta^{-\frac{1}{4}} \ln^{\frac{1}{2}}(1/\delta) M^2 / ((1 - \lambda)^2 J M^2 x^\ddagger + J^2).\end{aligned}$$

Discussion. As already noted, the behaviour in the outer region is the same in all cases. However, from the practical point of view it is the variations of s that are of most significance, and these occur in the remaining (narrower) regions, the behaviour of the two mechanisms being significantly different. The transition between the two extremes is rather abrupt; the behaviour for $b < b_c$ is largely dissociative-controlled, while for $b > b_c$ much of the behaviour is kick-out-dominated. This transition occurs for $\varepsilon = O(\delta^{\frac{1}{2}})$, i.e. for much stronger kick-out contributions than the corresponding transition for in-diffusion, which occurs when $\varepsilon = O(\delta)$; see Part I.

5. Conclusions

The physical conditions required for out-diffusion can arise in a number of different ways; one relevant set of circumstances, to which we have already alluded, is related to the surface source in-diffusion problem discussed in Part I. Here the semiconductor is initially doped using a surface source of impurity, the whole system being held at high temperature. If the surface source is then removed, with the temperature of the system remaining sufficiently high, impurity will out-diffuse through the surface. The initial distribution of impurity in these circumstances will not be completely uniform, but treating more general initial conditions does not complicate the analysis significantly. In particular, the leading order outer equation for the interstitial impurity is unchanged when the initial conditions are modified, and the leading order outer substitutional concentration again remains constant in time. The analysis of the surface regions can also be generalised in, for the most part, a relatively straightforward fashion.

The leading order outer problem is almost identical in all the cases analysed above, with $s \sim 1$ for $x = O(1)$, but the different regimes are distinguished by their behaviour in regions near the surface. A particularly interesting case for the charged defect model arises when $\varepsilon = O(\delta^{1/2})$. Writing $\varepsilon = b\delta^{1/2}$, we have shown that the character of the diffusion behaviour differs between $b < b_c$ and $b > b_c$, where the constant b_c is defined by equation (4.13). For $b < b_c$ the behaviour is largely dissociative-controlled, while for $b > b_c$ kick-out effects play the more important role. It is noteworthy that this transition occurs at a particular (finite) value of b and for a scaling that has $\varepsilon \gg \delta$. For the in-diffusion charged defect model, the corresponding transition occurs on the scaling $\varepsilon = O(\delta)$; this distinction is not unexpected, since in-diffusion leads to an undersaturation of vacancies (reducing dissociative effects) whereas out-diffusion leads to a supersaturation (enhancing the dissociative contribution). Because of such differences, in-diffusion and out-diffusion experiments can yield distinct, and complementary, information about the mechanisms responsible for the diffusion of a given impurity.

It is worth remarking that, in the asymptotics, the expressions

$$p = \frac{s}{1-\lambda}, \quad \frac{\partial}{\partial x} \left(\frac{\partial i}{\partial x} - \frac{i}{p} \frac{\partial i}{\partial x} \right) = 0$$

hold to leading order in all cases in all the regions except the outer; they can thus simplify the analysis of the regions close to the semiconductor surface.

We conclude by making some comments comparing the various cases. A convenient way to characterise them is given by the following table, which summarises the behaviour of two of the key physical features. The maximum of V can occur either within a layer (marked (W)) or in the matching region between two layers (marked (M)); in the latter cases, an explicit leading order expression for the maximum can be deduced from the preceding analysis. We note that $I = 1/V$ holds in the neutral defect case, so the self-interstitial minimum can be inferred from the vacancy maximum; in the charged defect case we have $I = p^2/V$ and we believe the self-interstitial concentration to be monotonic increasing. This is an important qualitative distinction between cases (I) and (II). The middle column indicates the range of x over which $s \sim 1$ does not hold.

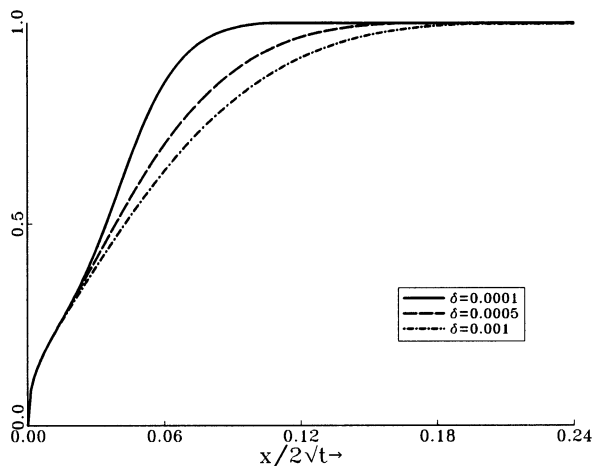


FIG. 8—Plots of the substitutional profile near the surface for the defect neutral model with various values of δ and $\beta = \gamma = 1$, $\varepsilon = 0.0025$, $\lambda = 0.4$, $\varpi = 0.0001$.

| | Range over which s varies | Maximum of V |
|--|--|--|
| Dissociative | $x = O(\delta^{1/3})$ | (W) $V = O(\delta^{-1/3})$ |
| (I) Kick-out | $x = O(\varepsilon^{1/2})$ | (M) $V = O(\varepsilon^{-1/3})$ |
| $\varepsilon = O(\delta^{5/6})$ | $x = O(\delta^{1/3}) = O(\varepsilon^{2/5})$ | (W) $V = O(\delta^{-1/3}) = O(\varepsilon^{-2/5})$ |
| $\varepsilon = O(\delta^{3/4})$ | $x = O(\delta^{3/8}) = O(\varepsilon^{1/2})$ | (M) $V = O(\delta^{-1/4}) = O(\varepsilon^{-1/3})$ |
| (II) Kick-out | $x = O(\varepsilon^{3/4} \ln^{1/4}(1/\varepsilon))$ | (M) $V = O(\varepsilon^{-1/2} \ln^{1/2}(1/\varepsilon))$ |
| $\varepsilon = b\delta^{1/2}, b < b_c$ | $x = O(\delta^{1/3}) = O(\varepsilon^{2/3})$ | (W) $V = O(\delta^{-1/3}) = O(\varepsilon^{-2/3})$ |
| $\varepsilon = b\delta^{1/2}, b > b_c$ | $x = O(\delta^{3/8} \ln^{1/4}(1/\delta))$ $= O(\varepsilon^{3/4} \ln^{1/4}(1/\varepsilon))$ | (M) $V = O(\delta^{-1/4} \ln^{1/2}(1/\delta))$ $= O(\varepsilon^{-1/2} \ln^{1/2}(1/\varepsilon))$ |

The extent of vacancy supersaturation is therefore decreased by increasing the kick-out contribution (cf. Figs 4 and 7). For the same ε , the range of x over which s varies significantly is much less in case (II) than in case (I), provided δ is sufficiently small that dissociative effects do not dominate (we recall that the dissociative limit is the same in both cases). These predictions are confirmed by the numerical results for the substitutionals displayed in Figs 8 and 9. The profiles change significantly as b varies close to b_c , but we shall not discuss transition scalings with $b - b_c = o(1)$, since such a regime would be very hard to investigate experimentally. Finally, we remark on the decrease in the vacancy supersaturation as b rises through b_c . Through the surface region (4.4.2(i) or 4.4.3(i)), the surface acts as a vacancy sink, extracting some of the excess vacancies generated in the bulk. This region is kick-out-controlled (see (4.2)), and increasing kick-out effects by increasing b through b_c has a surprisingly dramatic effect in increasing the size of this region, making it more effective in extracting vacancies from the bulk. The moving boundary problem (4.15) can be viewed as a representation of this vacancy extraction process. We should note,

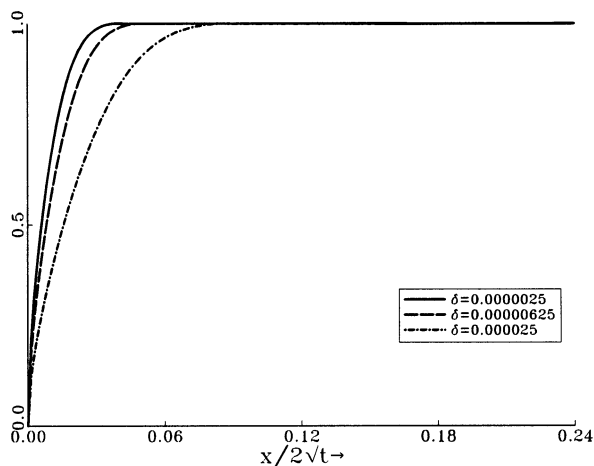


FIG. 9—Plots of the substitutional profile near the surface for the charged neutral model with various values of δ and $\beta = \gamma = 1$, $\varepsilon = 0.0025$, $\lambda = 0.4$, $\varpi = 0.0001$. The three curves correspond to the values $b = 1.5811, 1.0$ and 0.5 ; recall that $b_c \approx 0.75$ here.

however, that, unless δ is unusually small, $\delta^{-1/3}$ is not in practice significantly larger than $\delta^{-1/4} \ln^{1/2}(1/\delta)$.

Some remarks about effective diffusivities are in order. In the neutral defect case

$$D(s) = \frac{2\beta\delta^{3/4}s}{(q_0^*J(1-\lambda)^2)^{2/3}} + \frac{2\gamma b(q_0^*J(1-\lambda)^2)^{2/3}\delta}{s^3} \quad (5.1)$$

gives an expression for the effective substitutional diffusivity that is valid to leading order in both layer (ii) and layer (iii) of case (B) in Section 3.4. The first term in (5.1) (the dissociative contribution) is of ‘slow’ diffusion type, vanishing at $s = 0$, while the second (the kick-out contribution) is a ‘fast’ diffusion term, blowing up as $s \rightarrow 0$. The interaction between the two can be regarded as responsible for the somewhat complicated asymptotic structure described above, and the non-local dependence on the unknown $q_0^*(t)$ should be stressed. Similarly, from regions (ii) and (iii) in Section 4.4.3 we obtain the corresponding expression

$$D(s) = \frac{2\beta\delta^{3/4}M^2s}{J} + \frac{2\gamma bJ^2\delta^{3/4}\ln^{-1}(1/\delta)}{M^2(1-\lambda)^2s}; \quad (5.2)$$

this also has non-local dependence, through $M(t)$. The ‘slow’ diffusion (dissociative) term of (5.2) is equivalent to that of (5.1), but the power law in the ‘fast’ (kick-out term) has increased from -3 to -1 , and this change can be viewed as being responsible for most of the differences in asymptotic structure between case (I) and case (II). Experimental measurements of effective diffusivities, using the Boltzmann–Matano approach, for example, could conveniently be assessed against expressions such as (5.1)–(5.2), and information about which charge states dominate could be gleaned thereby.

We conclude by noting that a similar phenomenon can occur in much simpler systems; we consider a related problem for the very widely studied porous medium equation, namely,

$$\begin{aligned} \frac{\partial c}{\partial t} &= \frac{\partial}{\partial x} \left(c \frac{\partial c}{\partial x} \right), \\ c &= 1 \quad \text{at} \quad t = 0, \\ c &\rightarrow 1 \quad \text{as} \quad x \rightarrow +\infty. \end{aligned} \tag{5.3}$$

If we close the system by imposing the flux condition

$$c \frac{\partial c}{\partial x} = \mu t^{-1/2} \quad \text{at} \quad x = 0, \tag{5.4}$$

where μ is a constant and the time dependence is chosen to achieve self-similarity, the solution $c(x/\sqrt{t})$ is strictly positive for sufficiently small μ . However, a bifurcation in the behaviour occurs at $\mu = \mu_c > 0$, where μ_c is determined by solving (5.3) subject to

$$c = 0 \quad \text{at} \quad x = 0$$

and then evaluating

$$\mu_c = \lim_{x \rightarrow 0} t^{1/2} c \frac{\partial c}{\partial x}.$$

For $\mu > \mu_c$ the condition (5.4) cannot be imposed on non-negative solutions; rather, if we wish to extract material at the rate $\mu t^{-1/2}$, this should be done at a moving boundary $x = vt^{1/2}$ with

$$c = 0, \quad c \frac{\partial c}{\partial x} = \mu t^{-1/2} \quad \text{at} \quad x = vt^{1/2}, \tag{5.5}$$

where the positive constant v is determined as part of the solution, giving $v \rightarrow 0$ as $\mu \rightarrow \mu_c^+$; (5.5) could also be imposed for $\mu < \mu_c$, but one would then obtain $v < 0$. Writing $s(t) = vt^{1/2}$ for $v > 0$, so that $c(x, t) = 0$ for $0 \leq x \leq s(t)$ and the non-linear diffusion equation holds in $x > s(t)$, one thus has

$$s(t)c(0, t) = 0 \quad \text{with} \quad s(t) \geq 0, \quad c(0, t) \geq 0,$$

with $s(t) = 0$ for $\mu < \mu_c$ and $c(0, t) = 0$ for $\mu > \mu_c$. Such a prescription corresponds to a diffusivity

$$\begin{aligned} D(c) &= c \quad \text{for} \quad c > 0, \\ &= \infty \quad \text{for} \quad c = 0, \end{aligned}$$

which amounts to a limit case of (5.2). A natural generalisation involves allowing the right-hand side of (5.4) to be any specified function of t ; such problems are of some mathematical novelty and interest, cf. [1].

ACKNOWLEDGEMENTS

We are grateful to the British Council/Enterprise Ireland for the award of travel grants. JRK is grateful to the Leverhulme Trust for support, and MGM to Forbairt for the award of a basic research grant.

REFERENCES

- [1] G.I. Barenblatt and J.L. Vazquez, A new free boundary problem for unsteady flows in porous media, *European Journal of Applied Mathematics* **9** (1998), 37–54.
- [2] J. Crank, *The mathematics of diffusion*, Clarendon, Oxford, 1956.
- [3] S. Yu, T.Y. Tan and U. Gosele, Diffusion mechanism of chromium in GaAs, *Journal of Applied Physics* **70** (1991), 4827–36.